

AD-A094 901

UNIVERSAL ENERGY SYSTEMS INC DAYTON OHIO

F/G 20/11

USE OF REISSNER'S VARIATIONAL PRINCIPLE IN FINITE ELEMENT ANALY-ETC(U)

DEC 80 J AHMAD

F33615-79-C-5129

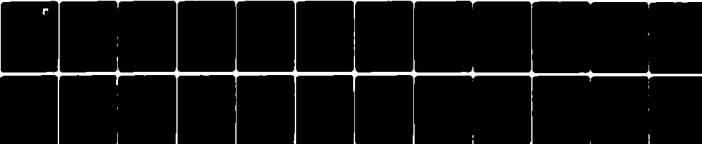
UNCLASSIFIED

AFWAL-TR-80-4182

NL

1 of 1

ADA
09-2001

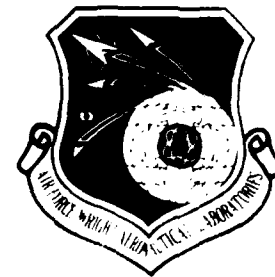


END
DATE
FILMED
3-81
DTIC

AFWAL-TR-80-4182

SECRET

20



AD A094901

USE OF REISSNER'S VARIATIONAL PRINCIPLE IN FINITE ELEMENT ANALYSIS OF CRACK PROBLEMS

Jalees Ahmad

Metals Behavior Branch
Metals and Ceramics Division

December 1980

TECHNICAL REPORT AFWAL-TR-80-4182

Final Report for Period June 1980 - September 1980

Approved for public release; distribution unlimited.

DDC FILE COPY

MATERIALS LABORATORY
AIR FORCE WRIGHT AERONAUTICAL LABORATORIES
AIR FORCE SYSTEMS COMMAND
WRIGHT-PATTERSON AIR FORCE BASE, OHIO 45433

01 2 11 231

NOTICE

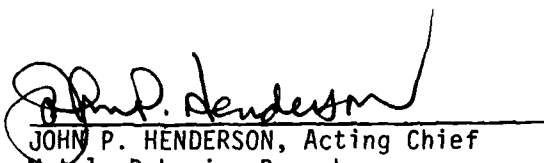
When Government drawings, specifications, or other data are used for any purpose other than in connection with a definitely related Government procurement operation, the United States Government thereby incurs no responsibility nor any obligation whatsoever; and the fact that the government may have formulated, furnished, or in any way supplied the said drawings, specifications, or other data, is not to be regarded by implication or otherwise as in any manner licensing the holder or any other person or corporation, or conveying any rights or permission to manufacture, use, or sell any patented invention that may in any way be related thereto.

This report has been reviewed by the Office of Public Affairs (ASD/PA) and is releasable to the National Technical Information Service (NTIS). At NTIS, it will be available to the general public, including foreign nations.

This technical report has been reviewed and is approved for publication.



THEODORE NICHOLAS, PROJECT ENGINEER



JOHN P. HENDERSON, Acting Chief
Metals Behavior Branch
Metals and Ceramics Division

"If your address has changed, if you wish to be removed from our mailing list, or if the addressee is no longer employed by your organization please notify AFWAL/MLLN, W-PAFB, OH 45433 to help us maintain a current mailing list".

Copies of this report should not be returned unless return is required by security considerations, contractual obligations, or notice on a specific document.

REPORT DOCUMENTATION PAGE		READ INSTRUCTIONS BEFORE COMPLETING FORM	
1. REPORT NUMBER AFWAL/TR-80-4182	2. GOVT ACCESSION NO. AD-A094901	3. RECIPIENT'S CATALOG NUMBER 91	
4. TITLE (and Subtitle) USE OF REISSNER'S VARIATIONAL PRINCIPLE IN FINITE ELEMENT ANALYSIS OF CRACK PROBLEMS		5. TYPE OF REPORT & PERIOD COVERED June 1980 - September 1980	
7. AUTHOR(s) Jalees Ahmad		6. PERFORMING ORG. REPORT NUMBER	
9. PERFORMING ORGANIZATION NAME AND ADDRESS Materials Laboratory (AFWAL/MLLN) Air Force Wright Aeronautical Laboratories (AFSC) Wright-Patterson Air Force Base, Ohio 45433		10. PROGRAM ELEMENT, PROJECT, TASK AREA & WORK UNIT NUMBERS 2307P102	
11. CONTROLLING OFFICE NAME AND ADDRESS Materials Laboratory (AFWAL/MLLN) Air Force Wright Aeronautical Laboratories (AFSC) Wright-Patterson Air Force Base, Ohio 45433		12. REPORT DATE December 1980	
14. MONITORING AGENCY NAME & ADDRESS (if different from Controlling Office)		13. NUMBER OF PAGES 31	
		15. SECURITY CLASS. (of this report) Unclassified	
		15a. DECLASSIFICATION DOWNGRADING SCHEDULE	
16. DISTRIBUTION STATEMENT (of this Report) Approved for public release; distribution unlimited.			
17. DISTRIBUTION STATEMENT (of the abstract entered in Block 20, if different from Report)			
18. SUPPLEMENTARY NOTES			
19. KEY WORDS (Continue on reverse side if necessary and identify by block number) Finite Element Method Linear Elastic Fracture Mechanics Reissner's Variation Principle Three-Dimensional Problems			
20. ABSTRACT (Continue on reverse side if necessary and identify by block number) For the purpose of accurately estimating linear elastic fracture parameters by finite element method, the use of Reissner's variational principle as a basis is investigated. Results of two-dimensional analyses performed on three-point bend, compact tension, and ring tension geometries compare well with other solutions available in the literature. Results of three-dimensional analyses of three-point bend and ring geometries are also presented. The method appears to be particularly useful in studying through the thickness variation or Mode I stress intensity factors.			

TABLE OF CONTENTS

SECTION	PAGE
I INTRODUCTION	1
II FORMULATION	3
III NUMERICAL EXAMPLES	8
1. Two-Dimensional Problems	9
a. Three-Point Bend Specimen	9
b. Compact Tension Specimen	9
c. Double Notch Ring Specimen	10
2. Three-Dimensional Problems	10
a. Three-Point Bend Specimen	10
b. Double Notch Ring Specimen	10
IV SUMMARY AND DISCUSSION	12
REFERENCES	13

LIST OF ILLUSTRATIONS

FIGURE		PAGE
1	Crack Tip Coordinates	19
2	A Typical Finite Element Mesh	20
3	Results for Three-Point Bend Specimen (Two-Dimensional)	21
4	Results for Compact Tension Specimen (Two-Dimensional)	22
5	Results for Ring Specimen (Two-Dimensional)	23
6	Three-Point Bend Specimen with Straight Crack Front	24

LIST OF TABLES

TABLE	PAGE
1 Results for Three-Point Bend Specimen (Two-Dimensional)	14
2 Results for Compact Specimen (Two-Dimensional)	15
3 Finite Element Results for Ring Geometry (Two-Dimensional)	16
4 Results for Three-Point Bend Specimen (Three-Dimensional)	17
5 Results for Ring Specimen (Three-Dimensional)	18

SECTION I

INTRODUCTION

In Solid Mechanics, the most widely used variational principles are the virtual displacement principle, the complementary energy principle, and Reissner's variational principle (Reference 1). In finite element stress analysis the virtual displacement principle is most commonly used; providing the usual displacement based elements. The complementary energy principle has also been to some extent exploited (Reference 2). The third, and the most general of the three variational principles, is Reissner's variational principle. Although this variational principle has remained largely unexploited in certain types of problems it proves to be quite useful (Reference 3).

The advantages gained by using Reissner's variational principle are significant when the problems are such that precise point wise stress and strain distributions are required. Also in problems where satisfaction of nodal force equilibrium needs to be repeatedly checked, such as in non-linear material problems, Reissner's principle is advantageous. The most outstanding advantage in using Reissner's principle is that the continuity requirements on the choice of shape functions are somewhat relaxed (Reference 4).

The disadvantages associated with the use of Reissner's principle need also to be emphasized. Firstly, the mathematical foundations of finite element formulation based on this principle are not as strong (References 1-4) as in the case of displacement based elements. Much work regarding the proof and convergence of the method still needs to be done. The second disadvantage is that the assembled coefficient matrix in this formulation is not as well behaved as in the case of displacement formulation (Reference 5).

The purpose of this report is to outline the salient features of the numerical formulation of finite element method based on Reissner's

AFWAL-TR-80-4182

variational principle. Numerical examples, mainly of crack problems, are presented. Some two- and three-dimensional analysis results can be useful in fracture mechanics. Comparison with available analytical results is provided.

SECTION II
FORMULATION

Reissner's variational principle is distinguished by the first variation of the functional J_R being equal to zero, i.e.,

$$\delta J_R = 0 \quad (1)$$

where

$$J_R = \int_v \left\{ -W_c(\sigma_{ij}) - F_i U_i + \frac{1}{2} \sigma_{ij} (U_{i,j} + U_{j,i}) \right\} dv - \int_{S_\sigma} T_{i*} U_i ds - \int_{S_u} \sigma_{ij} v_i (U_i - U_{i*}) ds \quad (2)$$

in which

- W_c is complementary energy function
- σ_{ij} is stress tensor
- U_i are displacement components
- $U_{i,j}$ is partial derivative of U_i with respect to j
- F_i are body forces per unit volume
- T_{i*} are surface forces per unit area
- v_i are direction cosines of the surface normal
- U_{i*} are prescribed displacements on S_u
- S_u is that portion of the boundary on which displacements are prescribed
- S_σ is that portion of the boundary on which stresses are prescribed
- v is the domain.

Taking the first variation of J_R and equating it to zero one can obtain the basic equations of elasticity (Reference 6). In simpler terms the principle can be stated as follows:

$$J_R = U + V \quad (3)$$

where

- J_R = Total potential energy
- U = Strain energy
- V = Potential energy due to applied loads

In the absence of initial strains and body forces

$$U = \int_V [\sigma][\epsilon] dv - U^*$$

where, U^* is complementary strain energy. Therefore,

$$J_R = \int_V [\sigma][\epsilon] dv - U^* + V \quad (4)$$

Use of Equation 1 over a subdomain (element) leads to the following matrix equation:

$$[K][\alpha] = [F] \quad (5)$$

where

$$[K] = \begin{bmatrix} -[K_{11}] & : & [K_{12}] \\ n \times n & \cdot & n \times m \\ \cdot & \cdot & \cdot \\ [K_{12}]^T & : & [0] \\ m \times n & \cdot & m \times m \end{bmatrix} \quad [\alpha] = \begin{bmatrix} [\sigma] \\ n \times 1 \\ \cdot \\ [r] \\ m \times 1 \end{bmatrix}, \quad [F] = \begin{bmatrix} [F_\sigma] \\ n \times 1 \\ \cdot \\ [F_r] \\ m \times 1 \end{bmatrix}$$

$$[K_{11}] = \int_V [Z]^T [D]^{-1} [Z] dv \quad (6)$$

$$[K_{12}] = \int_v [Z]^T [B] dv - \int_{s_u} [L]^T [Y] ds \quad (7)$$

$$[F_r] = \int_{s_\sigma} [Y]^T [T] ds, [F_\sigma] = \int_{s_u} [Y]^T [U] ds \quad (8)$$

[B] is strain-nodal displacement relationship matrix

[Z] is stress-nodal stress relationship matrix

[L] is boundary traction-nodal force relationship matrix

[D] is stress-strain constitutive relationship matrix

[Y] is boundary displacement nodal displacement relationship matrix

[T] is boundary traction vector

[U] is boundary displacement vector

[r] is nodal displacement vector

[σ] is nodal stress tensor written in vector form

The element matrix (Equation 5) is then used to form the master coefficient matrix employing the usual finite element assembly procedure. A noticeable feature of Equation 5 is that nodal stress components along with the nodal displacement components appear as primary unknowns of the problem.

Further, [B] and [Z] matrices appear unrelated and therefore, interpolation functions for displacement and stresses can be chosen quite independently. This provides increased flexibility to the computer code in terms of improving stress estimates. As for the satisfaction of equilibrium and compatibility equations of elasticity, they are both satisfied in an integral sense. This in turn relaxes the constant derivative requirement on the shape functions (Reference 1).

By simple block matrix rules one can write Equation 5 as follows:

$$-[K_{11}][\sigma] + [K_{12}][r] = [F_\sigma] \quad (9)$$

and

$$[K_{12}]^T [\sigma] = [F_r] \quad (10)$$

from Equation 10 it is then possible to recover the force vector F_r ; a procedure which is commonly necessary in problems involving nonlinear material behavior.

For application to problems in linear elastic fracture mechanics, commonly sought parameters are the stress intensity factors (Reference 7). The Mode I stress intensity factor (K_I) can be found by using the following equations:

$$\begin{aligned} \sigma_x = & \frac{K_I}{\sqrt{2\pi r}} \cos \frac{\theta}{2} [1 - \sin \frac{\theta}{2} \sin \frac{3\theta}{2}] - \frac{K_{II}}{\sqrt{2\pi r}} \sin \frac{\theta}{2} \\ & [2 + \cos \frac{\theta}{2} \cos \frac{3\theta}{2}] + \dots \end{aligned} \quad (11)$$

$$\begin{aligned} \sigma_y = & \frac{K_I}{\sqrt{2\pi r}} \cos \frac{\theta}{2} (1 + \sin \frac{\theta}{2} \sin \frac{3\theta}{2}) + \frac{K_{II}}{\sqrt{2\pi r}} \sin \frac{\theta}{2} \\ & \cos \frac{\theta}{2} \cos \frac{3\theta}{2} + \dots \end{aligned} \quad (12)$$

or, alternatively by

$$\begin{aligned} U = & \frac{K_I}{G} \left(\frac{r}{2\pi} \right)^{1/2} \cos \frac{\theta}{2} [1 - 2p + \sin^2 \frac{\theta}{2}] \\ & + \frac{K_{II}}{G} \left(\frac{r}{2\pi} \right)^{1/2} \sin \frac{\theta}{2} [2 - 2p + \cos^2 \frac{\theta}{2}] + \dots \end{aligned} \quad (13)$$

$$\begin{aligned} V = & \frac{K_I}{G} \left(\frac{r}{2\pi} \right)^{1/2} \sin \frac{\theta}{2} [2 - 2p - \cos^2 \frac{\theta}{2}] \\ & + \frac{K_{II}}{G} \left(\frac{r}{2\pi} \right)^{1/2} \cos \frac{\theta}{2} [-1 + 2p + \sin^2 \frac{\theta}{2}] + \dots \end{aligned} \quad (14)$$

where U and V are X and Y components of displacements near the crack tip.
 G is shear modulus and

$$\begin{aligned} \mu &= \nu = \text{Poisson's ratio for plane strain conditions} \\ &= \frac{\nu}{1 + \nu} \quad \text{for plane stress conditions.} \end{aligned} \quad (15)$$

The crack-tip coordinate system is shown in Figure 1. In the evaluation of stress intensity factors Equations 13 and 14 are commonly used. However, an extrapolation of values is usually necessary to arrive at accurate results. Further, in three-dimensional problems it becomes difficult to ascertain which value of μ should be chosen to represent the actual situation.

In the formulation presented earlier, Equations 11 and 12 can be conveniently used since accurate determination of nodal stress values is possible.

SECTION III

NUMERICAL EXAMPLES

The formulation presented previously can be used to develop a variety of finite element solution techniques by choosing various combinations of displacement and stress interpolation functions. Suitable interpolation functions can be chosen for particular applications and desired accuracy results.

For application to problems in linear elastic fracture mechanics, it was determined through numerical experimentation that parabolic shape functions for displacements and linear interpolation functions (Reference 2) for stress components provide accurate results both in two- and three-dimensional problems.

The numerical examples presented in the following were solved by using eight node quadrilateral and 20 node brick elements for the two- and three-dimensional cases considered. This procedure provided the displacement and stress components at each node from which other quantities of interest (K_I , crack opening displacement, etc.) were obtained.

In the illustrative examples that follow, three different fracture toughness test specimen configurations are presented. An extensive study of the effect of element size in the region surrounding the crack tip was conducted and the results indicated that by keeping the major element dimension at one-fifteenth of the crack length the error between the computed K_I values and the reference K_I values was consistently minimum (0.1 to 5.0%). In all the examples presented here the size of the elements surrounding the crack tip was therefore taken to be $(a/50.0)$, where "a" denotes the crack length.

For two-dimensional problems, K_I was evaluated by using the transverse displacement (V) of the node closest to the crack tip at $\theta = 180^\circ$ and by employing Equation 14. For three-dimensional problems, Equation 12 was

used by substituting the transverse stress (σ_y) at $\theta = 0.0$ and $r = (a/50.0)$. In all the examples Poisson's ratio of 0.3 was assumed. For two-dimensional problems plane stress conditions were assumed.

All the results are presented in nondimensional form. Nondimensional stress intensity factor (Y), and nondimensional crack opening compliance (C), and nondimensional load-line compliance (δ) are defined separately for each case considered. In the solutions British units were employed and specimen thickness (B) was assumed to be unity.

1. TWO-DIMENSIONAL PROBLEMS

a. Three-Point Bend Specimen

For the three-point bend specimen shown in Figure 3, a typical finite element mesh is shown in Figure 2. The problem was solved for a/W ratio ranging from 0.3 to 0.8. The results for nondimensional stress intensity factors (Y) and nondimensional load point compliance (δ) are shown in Figure 2. The referenced values were obtained from Reference 8. Crack opening compliance values measured at gage point (C_g) and at the notch mouth (C_m) are included in Table 1.

b. Compact Tension Specimen

Dimensions of the standard compact tension specimen are shown in Figure 4. The results for a/W of 0.3 to 0.8 were obtained by the present method.

The reference values for Y and $C(1-1)$ were obtained from Reference 8. The load at the pin hole was assumed to be sinusoidally distributed. In Table 2 the previous results and compliance values $C(m-m)$, $\delta(p-p)$, and $\delta(g-g)$ at measured locations m , p , and q , respectively, are included. This table also shows the effect of applying a concentrated load at point p .

c. Double Notch Ring Specimen

The geometry of a doubly notched ring under diametrically opposed concentrated tensile forces is shown in Figure 5. This specimen can be useful in studying the crack behavior in thick shell type structures usually encountered in nuclear power plant, gun-barrels, and in other applications. Nondimensional values for stress intensity factor and compliances at measurement locations 1, 2, and at the crack mouth are shown in Figure 5. Table 3 shows the actual finite element values.

2. THREE-DIMENSIONAL PROBLEMS

a. Three-Point Bend Specimen

The same three-point bend specimen of Figure 3 was analyzed using the three-dimensional formulation presented earlier. Due to double symmetry about X and Z axes (Figure 6), only one-quarter of the specimen was used in the analysis. Constant pressure loading consistent with the displacement interpolation functions was applied. The problem was solved for only one a/W ratio of 0.375.

Table 4 gives the variation of Y , C_m , and δ across the thickness (B) of the specimen. The definition of nondimensional quantities is consistent with Figure 3. The corresponding plane strain Y value for the crack length considered is 7.335 (Reference 8).

b. Double Notch Ring Specimen

A double notch ring specimen of 1.0 in thickness (B) and 0.5 in crack length (A) was analyzed using the three-dimensional formulation. Inner and outer radii of the ring were chosen to be 1.0 in. and 2.0 in., respectively. Due to symmetry about X, Y, and Z axes only one-eighth of the ring with appropriate boundary conditions needed to be considered. Consistent constant pressure load was applied along the inner radius at right angles to the crack line (Figure 5). Half the thickness of the ring was divided into two layers of brick elements.

AFWAL-TR-80-4182

The variations of K_I , crack opening displacement, and load line displacements across the ring thickness are given in Table 5. Notations are consistent with Figure 5.

SECTION IV

SUMMARY AND DISCUSSION

Two- and three-dimensional finite element formulations based upon Reissner's variational principle were described and applied to three different fracture toughness specimen geometries. For the three-point bend specimen and compact tension specimen the results of K_I and load line displacements agreed well with available two-dimensional analytical solutions. In general, the results for the compact specimen were found to be more accurate. One reason for the three-point bend specimen results being consistently higher than the corresponding reference values can be the effect of wedge action (Reference 9). This wedge action is characterized by a horizontal force of magnitude (P/π) being introduced at the load point when a concentrated force is split in half to solve geometrically symmetrical problems. For further information on wedge action, the reader is referred to References 9 and 10. For the double notch ring specimen geometry it is observed that K_I varies linearly with nondimensional crack lengths at 0.3 and 0.8. This observation can be useful in designing test specimens for use in parametric crack growth studies.

For the three-dimensional cases considered, it was found that for a three-point bend specimen with straight crack front the value of K_I is considerably lower (23%) at the specimen surface than at the middle plane. This fact can be useful in understanding the phenomenon of crack front "tunneling" in thick specimens. In the case of ring specimen, using the same Poisson's ratio ($= 0.3$), the variations in K_I , C , and δ follow the same variation as in the three-point bend specimen.

REFERENCES

1. Y. C. Fung, Foundations of Solid Mechanics, Prentice-Hall, 1965.
2. H. C. Martin and G. F. Carey, Introduction to Finite Element Analysis, McGraw-Hill, 1971.
3. K. J. Bathe and E. L. Wilson, Numerical Methods in Finite Element Analysis, Prentice-Hall, 1976.
4. O. C. Zienckiwicz, The Finite Element Method in Engineering Science, McGraw-Hill, 1971.
5. R. H. Gallagher, Finite Element Analysis Fundamentals, Prentice-Hall, 1975.
6. E. Reissner, "On a Variational Theory in Elasticity," J. Math. Phys. 29, 1950.
7. D. Broek, Elementary Engineering Fracture Mechanics, Noordhoff, 1974.
8. J. E. Srawley, "Wide Range Stress Intensity Factor Expressions for ASTM E 399 Standard Fracture Toughness Specimens," Int. J. Fract. 12, 1976.
9. S. Timoshenko and J. N. Goodier, Theory of Elasticity, McGraw-Hill, 1951.
10. E. A. Rippergen and N. Davis, "Critical Stresses in Circular Ring," Trans. ASCE 112, 1947.

TABLE 1
RESULTS FOR THREE-POINT BEND SPECIMEN (TWO-DIMENSIONAL)

a/w	PRESENT METHOD				REFERENCE 8	
	Y	δ	$C_g/2.0$	$C_m/2.0$	Y	δ
0.3	5.9150	31.4130	5.3072	5.3092	6.0849	28.9350
0.4	7.9128	41.1203	9.2696	9.2698	7.9273	38.6620
0.5	10.6892	58.0109	16.0276	16.0281	10.6500	55.6782
0.6	15.2798	90.0793	29.1007	29.0122	15.0864	88.1009
0.7	24.1313	160.7899	58.9445	58.9448	23.4014	159.5710
0.8	45.9050	367.0906	148.9148	148.9149	43.2129	366.1930

TABLE 3
FINITE ELEMENT RESULTS FOR RING GEOMETRY (TWO-DIMENSIONAL)

$A/R_0 - R_1$	γ	C/W	$\delta_1/2$	$\delta_2/2$
0.2	2.41187	1.44524	7.23047	5.27204
0.3	3.14134	2.34528	8.22151	6.23758
0.4	3.75508	3.42929	9.52616	7.51578
0.5	4.31905	4.77439	11.18300	9.14195
0.6	4.86283	6.46088	13.24592	11.16976
0.7	5.39278	8.56486	15.76643	13.65152
0.8	5.85839	11.11879	18.74005	16.58616

TABLE 4
RESULTS FOR THREE-POINT BEND SPECIMEN (THREE-DIMENSIONAL)

Z/B	Y	C_m	δ
0.0	7.3345	18.4378	80.0919
0.201	7.2799	18.4265	80.3194
0.402	6.6124	18.3780	81.2026
0.406	6.1522	18.3226	81.6613
0.500	5.6431	18.2424	82.2548

TABLE 5
RESULTS FOR RING SPECIMEN (THREE-DIMENSIONAL)

Z/B	Y	C/2	$\delta_1/2$	$\delta_2/2$
0.000	4.3214	4.3407	10.1740	8.3265
0.201	4.2899	4.3311	10.1992	8.3472
0.402	3.8897	4.3266	10.3109	8.4385
0.406	3.6246	4.3141	10.3693	8.4861
0.500	3.3193	4.2952	10.4428	8.5547

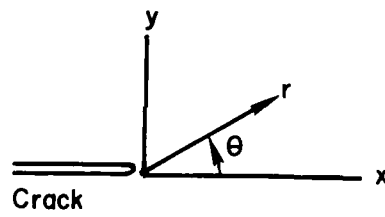


Figure 1. Crack Tip Coordinates

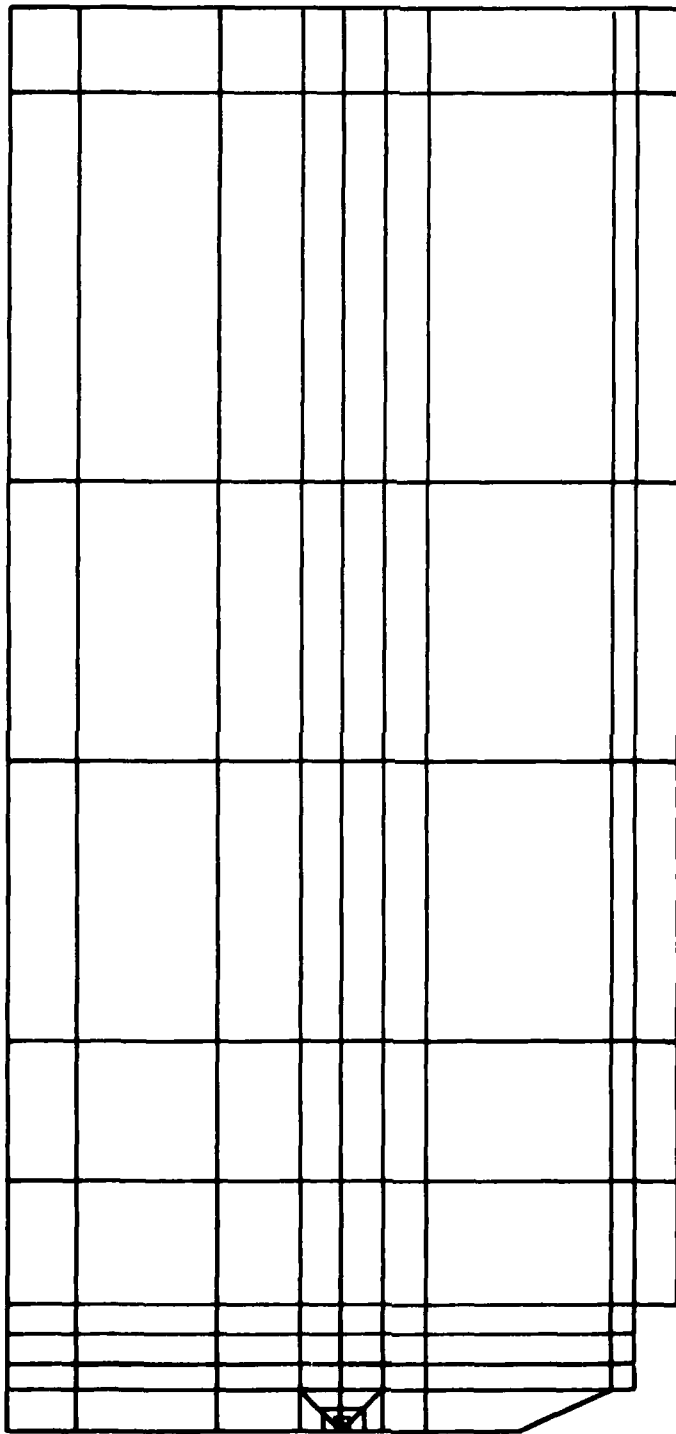
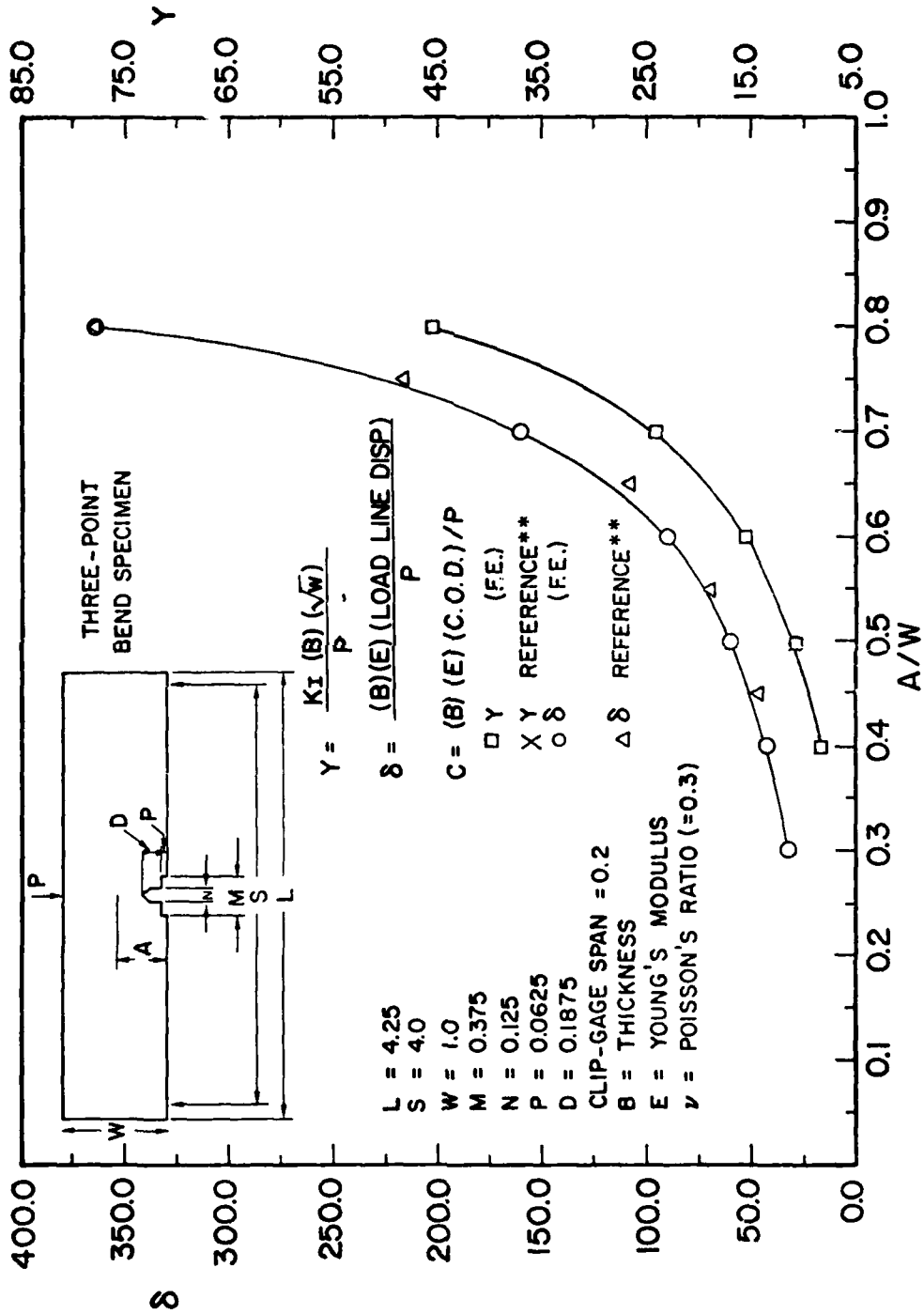
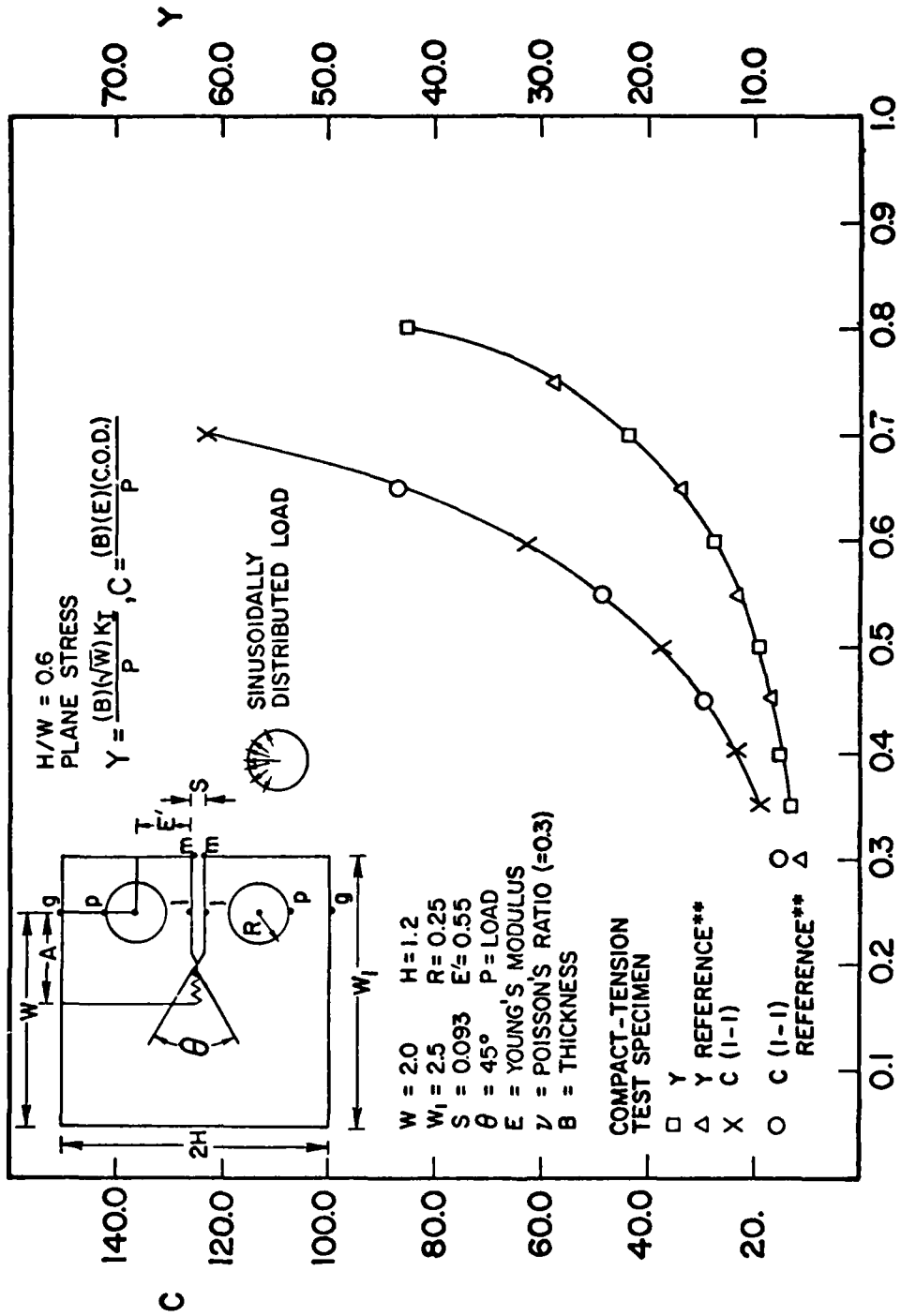


Figure 2. A Typical Finite Element Mesh



** SRAWLEY, INT. J. FRACT. 12, 475 (1976)

Figure 3. Results for Three-Point Bend Specimen (Two-Dimensional)



**SRAWLEY, INT. J. FRACT. 12, 475 (1976)

Figure 4. Results for Compact Tension Specimen (Two-Dimensional)

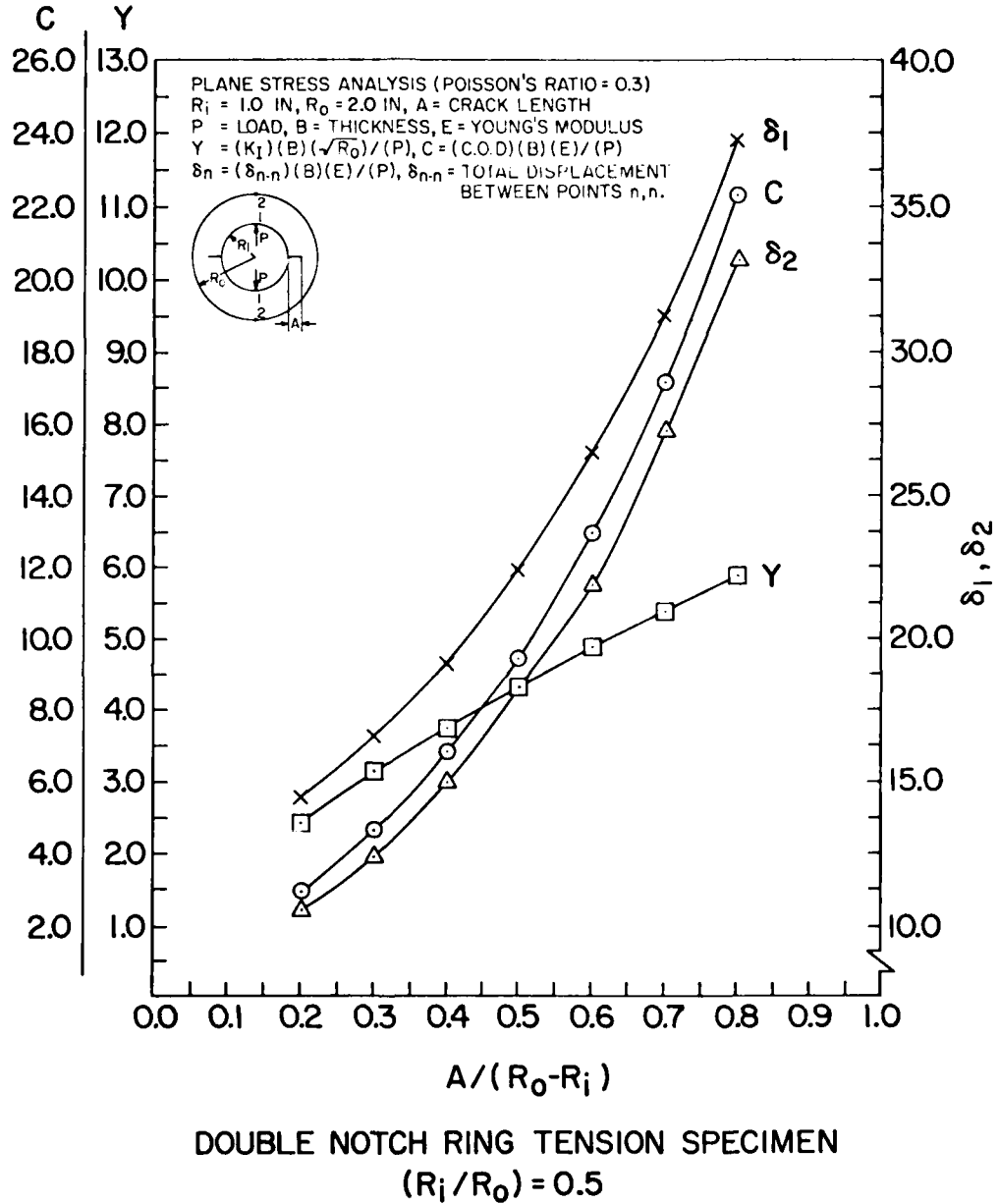


Figure 5. Results for Ring Specimen (Two-Dimensional)

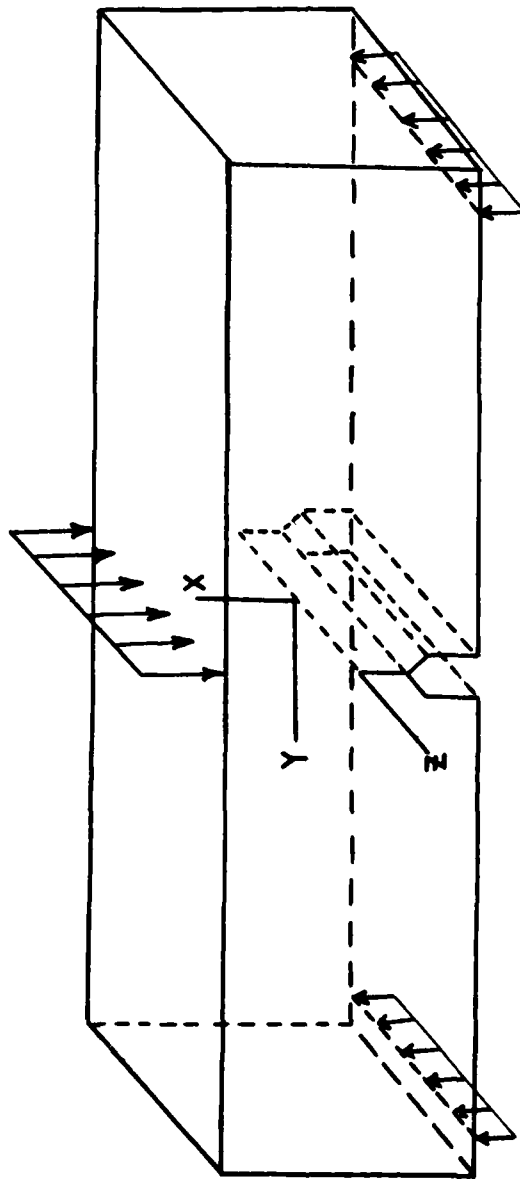


Figure 6. Three-Point Bend Specimen with Straight Crack Front

DATE
ILMED
—8